Mass Producible Low-Loss Broadband Optical Waveguides in Eagle2000 by Femtosecond Laser Writing

Vítor A. Amorim, Duarte Viveiros, João M. Maia, and P. V. S. Marques

***Abstract*— Optical waveguides were fabricated in alkaline earth boro-aluminosilicate glass, by femtosecond laser direct writing, with varying pulse energy and scan velocity. A spectral characterization, from 500 nm to 1700 nm, was made in order to determine their losses and understand its dependence on the processing parameters. Three major loss mechanisms were identified. At longer wavelengths, loss is mainly due to weak coupling. On the other hand, the behavior at shorter wavelengths is governed by propagation loss due to Rayleigh scattering, which was shown to be practically eliminated (<0.05 dB$\cdot$ cm$^{-1}\cdot$ μm^4) at higher scan velocities. Bulk absorption was also found to have an influence in the propagation losses at higher wavelengths. The combination of intermediate pulse energies (between 125-250 nJ) and high scan velocities (above 6 cm/s) allowed the fabrication of optical waveguides offering low losses across the entire range of wavelengths tested, facilitating applications that require larger wavelength working bands. Furthermore, since optimal fabrication conditions are achieved at higher scanning velocities, mass production with reduced fabrication times can be achieved.**

***Index Terms*— Coupling loss, low-loss broadband optical waveguides, femtosecond laser direct writing, integrated optics, mass production, Mie scattering, propagation loss, Rayleigh scattering.**

I. Introduction

THE possibility to directly inscribe optical waveguides in glasses using a femtosecond laser was first demonstrated by Davis *et al.* [1]. This technique differentiates itself from traditional photolithographic techniques, with prototyping flexibility (without the need for masks or multiple fabrication steps) and truly three-dimensional capabilities being its key advantages. However, it is a serial process, which translates into a lack of scalability and, therefore, higher costs, impeding its transition to a more mainstream technique in the fabrication of optical devices [2]. Fabrication times are, consequently, of the utmost importance in this regard. Fused silica has shown to be limited to scan velocities around 0.05 cm/s [3], limiting its applicability due to long manufacturing times. Alternative approaches, involving active beam shaping techniques through spatial light modulators, may enable batch fabrication and, thus, circumvent the serial processing nature of femtosecond laser writing [4]. Softer glasses like Corning Eagle2000 and Schott AF45 are also promising, allowing the fabrication of optical circuits at scan velocities around 2 cm/s [5]. In addition, these have better guiding properties at shorter wavelengths when compared to fused silica [3], [5], a region of the spectrum that is important in applications such as optical sensing utilizing plasmonics [6] and second harmonic generation [7], [8]. As such, understanding the losses of these waveguides and their dependence with fabrication parameters is vital to the improvement of the device's performance.

In this paper, we report a systematic study on the influence of pulse energy and scan velocity in the spectral characteristics, from 500 to 1700 nm, of optical waveguides embedded in alkaline earth boro-aluminosilicate glass (Eagle2000) using femtosecond laser direct writing. Coupling and propagation losses are presented, with the influence of Rayleigh and Mie scattering in the latter being explored, giving definitive insight on the impact of the writing parameters in such structures. An optimal processing window for the fabrication of low-loss broadband waveguides (in the entire range of wavelengths tested) was found at very high scan velocities (above 6 cm/s).

II. Experimental Procedure

A fiber amplified femtosecond laser (Satsuma HP, from Amplitude Systèmes), with a second harmonic beam at 515 nm and a pulse duration of approximately 250 fs at 1 MHz, was used to induce the refractive index modification in alkali-free boro-aluminosilicate glass (Eagle2000). Laser modification tracks were formed in a Workshop of Photonics Workstation by transverse scanning the substrate on Aerotech direct-drive stages (ANT130XY-110 PLUS and ANT130V-5 PLUS), with the linearly polarized beam focused at a depth of 100 μm via a 0.42 numerical aperture plan apochromat objective (Mitutoyo M Plan Apo NIR 50x). Laser beam polarization was set parallel to the writing direction, and all waveguides were written on the same scanning direction to avoid the Quill effect [9].

Manuscript received July 30, 2019; revised September 11, 2019; accepted September 15, 2019. Date of publication September 18, 2019; date of current version October 1, 2019. This work was supported in part by the Fundação para a Ciência e a Tecnologia under Grant SFRH/BD/128795/2017 and in part by the Project "On Chip Whispering Gallery Mode Optical Microcavities For Emerging Microcontaminant Determination In Waters" - SAFE WATER, which is supported and co-funded by the European Commission, Directorate-General Communications Networks, Content and Technology (DG CONNECT) under the ERA-NET Cofund scheme - Horizon 2020 "Horizon 2020 – the Framework Programme for Research and Innovation (2014–2020)". *(Corresponding author: Vítor A. Amorim.)*

The authors are with the CAP - Centre for Applied Photonics, INESC TEC, 4150-179 Porto, Portugal, and also with the Department of Physics and Astronomy, University of Porto, 4169-007 Porto, Portugal (e-mail: vitor.a.amorim@inesctec.pt; carlos.d.viveiros@inesctec.pt; joao.m.maia@inesctec.pt; psmarque@fc.up.pt).

Color versions of one or more of the figures in this letter are available online at http://ieeexplore.ieee.org.

Digital Object Identifier 10.1109/LPT.2019.2942104

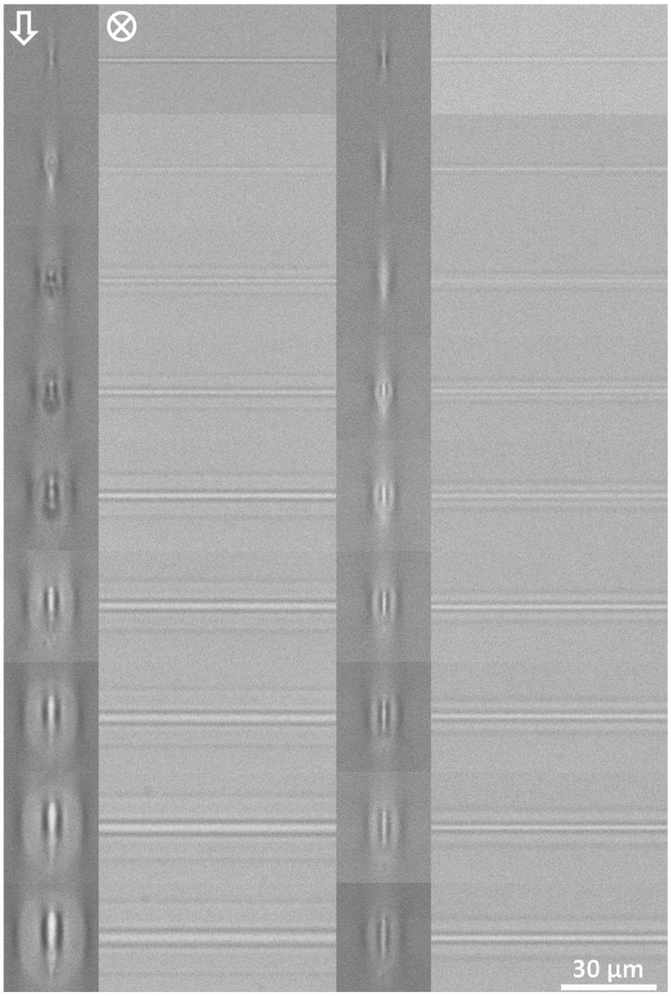

Fig. 1. Transmission mode optical microscope images of the cross-section and top views of waveguides written in fused silica with pulse energies of 50, 75, 100, 125, 150, 175, 200, 225, and 250 nJ (top to bottom, respectively), for a scan velocity of 1 cm/s (left) and 8 cm/s (right). Arrows indicate the laser beam propagation direction.

The side facets of all substrates were polished after writing. To determine the spectral characteristics of the waveguides, the broad spectrum of a halogen lamp was coupled into a single-mode fiber (SMF-28) and butt-coupled to the entrance facet of the modification tracks. The substrates were mounted on an Elliot Martock MDE881 stage with piezo controls (Dali E-2100) and special holders for precise alignment of the input/output optical fibers. The light collected by a second butt-coupled optical fiber at the exit facet was inspected in an optical spectrum analyzer (ANDO AQ-6315B) from 500 nm to 1700 nm with a 10 nm resolution. All transmission spectra were normalized to the source spectrum. Index matching (Cargille series: AA $n_D^{25°C} = 1.4580 \pm 0.0002$) was used to minimize Fresnel reflections at both input/output fibers/facets.

III. Experimental Results and Discussion

In this study, several optical waveguides were fabricated along a 75 mm long Eagle2000 substrate with pulse energy ranging from 50 nJ to 250 nJ and scan velocity between 1 cm/s to 8 cm/s. Fig. 1 displays the cross-section and top view of waveguides fabricated with different pulse energies for a scan velocity of 1 cm/s and 8 cm/s. As can be seen, these structures are composed by a central core delimited by a dark region and surrounded by an external cladding-like structure, which is typical for waveguides fabricated in the heat accumulation regime; both inner and outer-most regions are associated with a positive refractive index modification, that is greater in the center, with the dark region representing a negative refractive index modification [10], [11]. The dimensions of the modified volume are seen to increase significantly with pulse energy, diminishing for higher scan velocities, indicating a significant dependence on laser net fluence.

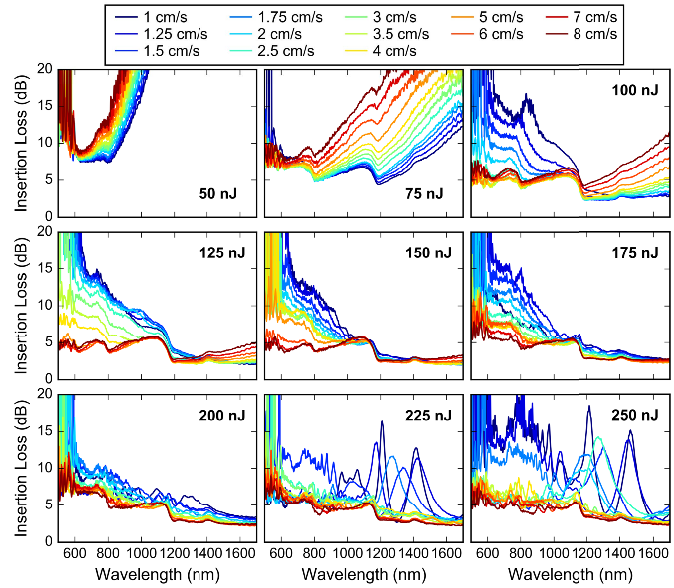

Fig. 2. Insertion loss of 2.3 cm long optical waveguides as a function of wavelength for varying pulse energy and scan velocity.

The spectral characteristics of the optical waveguides also depend on pulse energy and scan velocity, as can be seen in Fig. 2. At low pulse energies, a mid-wavelength guiding band delimited by increasingly higher insertion losses at shorter and longer wavelengths is observed. For pulse energies up to 150 nJ, insertion loss at longer wavelengths is seen to decrease monotonically with increasing pulse energy and decreasing scan velocity, region after which better results are achieved at higher scan velocity. The loss at shorter wavelengths is, on the other hand, maximized for intermediate pulse energies and smaller scan velocities, decreasing greatly for higher scan velocities independently of pulse energy. Furthermore, the spectrum of waveguides fabricated at high pulse energy (above 200 nJ) and low scan velocity (below 2.5 cm/s) is not as obvious as the remainder. The existence of peaks in the insertion loss spectrum can be explained by the presence of multiple waveguiding regions to which the light couples as it propagates.

To better understand the processes underlying the spectral behavior, the cut-back technique was used. In this study the substrates were diced into three different lengths (1.3, 2.3, and 3.2 ± 0.1 cm), with both propagation and coupling loss being retrieved from insertion loss fittings, as in [3].

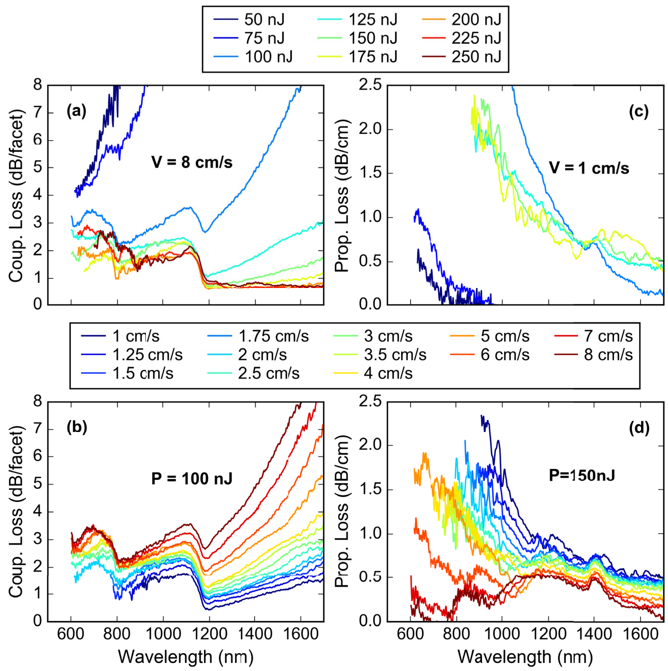

Fig. 3. Coupling and propagation loss as a function of wavelength for varying pulse energy (a, c) and scan velocity (b, d).

Waveguides fabricated at high pulse energy and low scan velocity were discarded from this analysis, as their complex behavior yielded results with considerable error.

Fig. 3 displays coupling and propagation losses for specific cases. From Fig. 3(a, b), it is possible to see that there are three main occurrences of interest. The first is the monotonic growth in coupling losses for longer wavelengths. This originates from the decrease in V-number, moving the guiding conditions closer to the cut-off condition and, therefore, increasing the mode field diameter, which translates into additional mode mismatch between the fiber and waveguide's mode. The second occurrence of interest is the variation in coupling losses, at longer wavelengths, with the fabrication parameters. We conclude that, at longer wavelengths, coupling losses increase whenever the pulse energy is decreased and/or the scan velocity increased. These results match our previous study developed in fused silica [3], and can be explained by the dependence of the refractive index modification as well as the dimensions of the guiding region in pulse energy and scan velocity, since these control the V-number. These are also in accordance with the behavior shown in Fig. 1, and allow the optimization of the coupling losses relative to the input fiber. The third is the existence of dips in the coupling loss spectra, as can be seen in Fig. 3(b) just before 800 nm and 1200 nm. These are related to the modal structure of the butt-coupling optical fibers, where each discontinuity corresponds to additional modes being supported at lower wavelengths. A more complex coupling behavior is also to be expected between optical waveguides fabricated with higher pulse energies and lower scan velocities, as these may support multiple modes at a given wavelength. Additionally, the coupling behavior will depend on the characteristics of the coupling optical fiber, meaning that different optical fibers will bear different results.

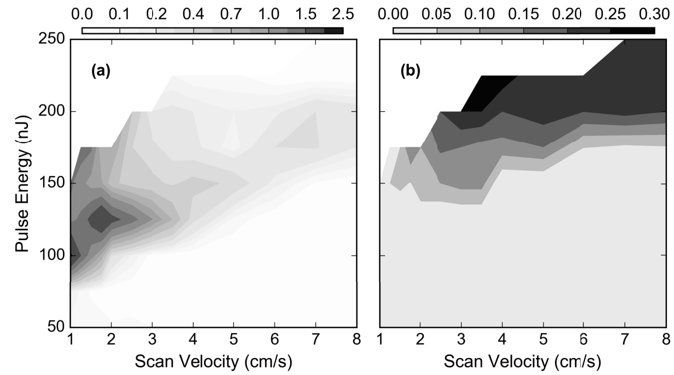

Fig. 4. Rayleigh (a) and Mie (b) scattering coefficients, in $\mathrm{dB \cdot cm^{-1} \cdot \mu m^4}$ and dB/cm respectively, as a function of pulse energy and scan velocity.

In Fig. 3(c), the monotonic increase in propagation loss, as wavelength decreases, is visible for all pulse energies tested; the steepness is also seen to depend on pulse energy. Such behavior was already observed in a previous study developed in fused silica [3], and was attributed to propagation loss being dominated by Rayleigh scattering. The propagation loss of such waveguides also depends on scan velocity, as can be seen in Fig. 3(d), with a significant decrease at shorter wavelengths being observed for higher scan velocities. Furthermore, small variations in the propagation loss spectra are seen to blue shift as scan velocity increases (Fig. 3(d)). These variations represent the appearance of additional propagation modes as wavelength decreases, since scattering affects different modes slightly differently, and their blue shift occurs due to a decrease in V-number from the decrease in refractive index contrast and waveguide dimensions. The same behavior occurs for decreasing pulse energy. Despite Rayleigh scattering being the major contributor to propagation loss, additional loss is also apparent from the C/λ^4 trend deviation, clearly seen in Fig. 3(d). This additional loss originates from the glass's bulk absorption [5], being created by the vibrational overtone of the hydroxyl group OH^- [12], with an absorption peak centered at 1385 nm, and by the ferrous ion Fe^{2+} [13], with a broad absorption peak at 1075 nm. An almost wavelength independent baseline loss also exists, which was attributed to Mie scattering.

Propagation loss, at longer wavelengths, is dominated by the bulk absorption of Eagle2000 ($BA_{Eagle2000}$) [5]. As such, in order to properly retrieve the Rayleigh and Mie scattering coefficients (C_{RS} and C_{MS}, respectively), the propagation loss data was modelled using equation (3), which takes the bulk absorption into account.

$$PL(\lambda) = \frac{C_{RS}}{\lambda^4} + C_{MS} + BA_{Eagle2000}(\lambda) \qquad (3)$$

The Rayleigh and Mie scattering coefficients are plotted in Fig. 4. It should be noted that the coefficients extracted from waveguides fabricated at low pulse energies and high scan velocities are estimated, as the large coupling loss variations at longer wavelengths give rise to higher propagation loss uncertainty. Rayleigh scattering, Fig. 4(a), is seen to decrease with scan velocity for all pulse energies tested, from a maximum of approximately 2 dB·cm$^{-1}\cdot\mu$m^4 to a negligible value at this scale (<0.05 dB·cm$^{-1}\cdot\mu$m^4). Pulse energy dependent behavior is also present, with higher Rayleigh scattering coefficients being found for waveguides fabricated at around 125 nJ and low scan velocity. This behavior is also perceptible from the transmission mode optical microscopy images present in Fig.1, where less light is seen to reach the end facet of waveguides fabricated with these parameters, improving for high scan velocities. The extracted Mie scattering coefficients are plotted in Fig. 4(b). From the data, an increase in the Mie scattering coefficient from $\approx$ 0 to 0.3 dB/cm is seen as pulse energy increases, being relatively independent of scan velocity. This behavior suggests that Mie scattering most likely arises from an energy dependent process. Curiously, there are no micrometer scale inhomogeneities visible within the waveguides, as seen in Fig. 1, that can explain these results.

The results obtained in this work are comparable to those achieved by Eaton *et al.* [14] in the telecommunications band while using the same material, where Rayleigh scattering coefficients ranging between 0.8 and 1.7 dB·cm$^{-1}\cdot\mu$m^4 and a Mie scattering coefficient of $\approx$0.16 dB/cm were found for a scan velocity between 0.8 and 2 cm/s and a pulse energy of 133 nJ at 1.5 MHz. As in this work, the authors found that the Mie scattering was independent of scan velocity and that the Rayleigh scattering decreases for higher scan velocity. Also, higher scan velocity meant that, in this work, we were able to reduce the Rayleigh scattering by an order of magnitude in relation to the results above. These results are also an improvement in relation to a previous study made in fused silica [3], as decreasing the Rayleigh scattering through thermal treatment increases the coupling losses at longer wavelengths dramatically. Mie scattering is also lower in the case of Eagle2000, with a two to three order of magnitude higher scan velocity being possible. Finally, the fabrication of low-loss broadband optical waveguides at scan velocities greater than 8 cm/s may still be achievable.

IV. Conclusion

The insertion losses of waveguides inscribed by femtosecond laser direct writing in alkaline earth boro-aluminosilicate glass substrates (Eagle2000) were characterized for different fabrication pulse energy and scan velocity. These presented a guiding band limited by increasingly higher losses at longer and shorter wavelengths. Coupling loss arising from the cut-off was found to control the long wavelength behavior, becoming negligible for pulse energies greater than 125 nJ. Added coupling loss due to modal mismatch was also present throughout the whole wavelength range. Regarding propagation loss, an almost wavelength independent baseline loss was observed, which was attributed to Mie scattering. The former showed to be relatively independent of scan velocity, increasing from $\approx$0 to 0.3 dB/cm as pulse energy increased. Bulk absorption was also present, being responsible for the majority of the propagation loss at longer wavelengths. On the other end, loss at shorter wavelengths is mostly determined by Rayleigh scattering, which was found to decrease with increasing scan velocity from approximately 2 dB·cm$^{-1}\cdot\mu$m^4 to a negligible value at this scale (<0.05 dB·cm$^{-1}\cdot\mu$m^4). In sum, the fabrication of low-loss broadband optical waveguides was achieved in Eagle2000, with optimal results being obtained for very high scanning velocities ($\approx$10 cm/s), facilitating the mass production of optical platforms employing such waveguides.

References

[1] K. M. Davis, K. Miura, N. Sugimoto, and K. Hirao, "Writing waveguides in glass with a femtosecond laser," *Opt. Lett.*, vol. 21, no. 21, pp. 1729–1731, Nov. 1996.

[2] M. Malinauskas *et al.*, "Ultrafast laser processing of materials: From science to industry," *Light Sci. Appl.*, vol. 5, no. 8, Aug. 2016, Art. no. e16133.

[3] V. A. Amorim, J. M. Maia, D. Viveiros, and P. V. S. Marques, "Loss mechanisms of optical waveguides inscribed in fused silica by femtosecond laser direct writing," *J. Lightw. Technol.*, vol. 37, no. 10, pp. 2240–2245, May 15, 2019.

[4] M. Sakakura, T. Sawano, Y. Shimotsuma, K. Miura, and K. Hirao, "Fabrication of three-dimensional 1 × 4 splitter waveguides inside a glass substrate with spatially phase modulated laser beam," *Opt. Express*, vol. 18, no. 12, pp. 12136–12143, Jun. 2010.

[5] T. Meany, S. Gross, N. Jovanovic, A. Arriola, M. J. Steel, and M. J. Withford, "Towards low-loss lightwave circuits for non-classical optics at 800 and 1,550 nm," *Appl. Phys. A, Solids Surf.*, vol. 114, no. 1, pp. 113–118, Jan. 2014.

[6] H. Y. Lin, W. H. Tsai, Y. C. Tsao, and B. C. Sheu, "Side-polished multimode fiber biosensor based on surface plasmon resonance with halogen light," *Appl. Opt.*, vol. 46, no. 5, pp. 800–806, Feb. 2007.

[7] H.-L. An, A. Arriola, S. Gross, A. Fuerbach, M. J. Withford, and S. Fleming, "Creating large second-order optical nonlinearity in optical waveguides written by femtosecond laser pulses in boro-aluminosilicate glass," *Appl. Phys. Lett.*, vol. 104, no. 2, Jan. 2014, Art. no. 021113.

[8] J. C. Ng, P. R. Herman, and L. Qian, "Second harmonic generation via femtosecond laser fabrication of poled, quasi-phase-matched waveguides in fused silica," *Opt. Lett.*, vol. 42, no. 2, pp. 195–198, Jan. 2017.

[9] P. G. Kazansky *et al.*, "'Quill' writing with ultrashort light pulses in transparent materials," *Appl. Phys. Lett.*, vol. 90, no. 15, Apr. 2007, Art. no. 151120.

[10] S. M. Eaton *et al.*, "Transition from thermal diffusion to heat accumulation in high repetition rate femtosecond laser writing of buried optical waveguides," *Opt. Express*, vol. 16, no. 13, pp. 9443–9458, Jun. 2008.

[11] A. Arriola *et al.*, "Low bend loss waveguides enable compact, efficient 3D photonic chips," *Opt. Express*, vol. 21, no. 3, pp. 2978–2986, Feb. 2013.

[12] O. Humbach, H. Fabian, U. Grzesik, U. Haken, and W. Heitmann, "Analysis of OH absorption bands in synthetic silica," *J. Non-Crystal. Solids*, vol. 203, pp. 19–26, Aug. 1996.

[13] L. B. Glebov and E. N. Boulos, "Absorption of iron and water in the Na_2O–CaO–MgO–SiO_2 glasses. II. Selection of intrinsic, ferric, and ferrous spectra in the visible and UV regions," *J. Non-Crystalline Solids*, vol. 242, no. 1, pp. 49–62, Dec. 1998.

[14] S. M. Eaton *et al.*, "Spectral loss characterization of femtosecond laser written waveguides in glass with application to demultiplexing of 1300 and 1550 nm wavelengths," *J. Lightw. Technol.*, vol. 27, no. 9, pp. 1079–1085, May 1, 2009.